Chapter

Corrosion and Natural Corrosion Inhibitors: A Case Study for *C. microphyllus*

Dwarika Prasad

Abstract

Worldwide, corrosion causes the value of the gross domestic product to decrease in industrialized countries by 4.26% and causes significant losses to industries including infrastructure. As a result, corrosion prevention and research related to it are extremely important. Some researchers are working to develop plant-based natural corrosion inhibitors, and experimental and computational studies are being conducted widely to prevent corrosion through cheap and environmental friendly coatings. A case study of *Convolvulus microphyllus* (*C. microphyllus*) extract was examined as eco-friendly for bio-corrosion inhibitor of mild steel in 0.5 M H_2SO_4 by using conventional weight loss, electrochemical polarization measurements, and electrochemical impedance spectroscopy (EIS) techniques. The compounds responsible for decreasing the rate of corrosion are kaempferol and phydroxycinnamic acid present in the extract. This inhibitor slows down the corrosion rate. Out of many observations, the best result 89.87% corrosion resistance efficiency was obtained at 600 mg/L of *C. microphyllus as* extract for mild steel in 0.5 M H_2SO_4 by applying electrochemical and weight loss measurements. The presence of a heteroatom in the main component of *C. microphyllus as* extract is believed to be an excellent inhibitor. Theoretical research revealed an entirely important report about comparative inhibition effect of different phytochemicals.

Keywords: adsorption, spontaneous reaction, natural inhibitors, electrochemical study, computational study

1. Introduction

The process of deposition of oxide layer on the surface of metals is called corrosion. It usually occurs when metal is exposed to moisture or water and gases such as dioxygen, dihydrogen, dichloride, hydrogen sulfide. It is a spontaneous chemical reaction with a slow rate. It usually occurs over days or weeks, and as a result of corrosion, the refined metal is turned into a more stable form such as oxide, hydroxide, or sulfide. The net worth of the corrosion prevention industry was estimated to be around $2.5 trillion (USD) in 2018 and is expected to cross $3.0 trillion (USD) by 2022, as per the National Association of Corrosion Engineers [1, 2]. The electrochemical phenomenon of degradation of material over course of time due to exposure toward the environment is called corrosion. Common types of corrosion for rusting of steel and internal polymeric pipeline are wet corrosion and dry corrosion [3]. In today's world, corrosion is no longer merely a chemical degradation

of metals, but also of semiconductive materials, insulating materials, and polymeric materials after exposure to the environment. It is a surface phenomenon, where at the material surface formed oxide or hydroxide or sulfide layer [4].

Mild steel is a low-priced material with properties that are suitable for most general engineering applications. That's why it is high in demand, but it contains very poor corrosion resistance. Corrosion produces very harmful effects on commercial industries such as paper mills, oil, and gas construction, and electronics used in a multitude of processes. When materials and structures are attacked by corrosion, they lose many of their useful properties. Some useful tools and machinery made from metal can become useless because of corrosion, many disaster situations such as chemical plant leaks, bridges can collapse and oil or gas pipelines can break and can produce a dangerous effect on the life of human beings. They also produce economical losses. Acid pickling is used for removing the impurities, scale, and sludge deposits on the metal surface. Acid pickling contains strong acid due to this, that process may cause a great economic loss. In the presence of inhibitors, the rate of acidic attack decreases on the metallic surface and it prevents metallic corrosion [5]. Decades of years many organic inhibitors, for example, phosphate esters, quaternary ammonium salts, amidoethyl imidazolines, as well as an inorganic inhibitor, for example, sulfate of Mg, Mn, Ni, and Zn are being used. Corrosion of steel has been inhibited by them. These types of inhibitors are generally costly and toxic and they might be harmful to the living organisms that is why the study of eco-friendly and non-toxic green inhibitors is important to prevent steel from corrosion nowadays. Natural corrosion inhibitors are biodegradable, non-toxic eco-friendly, and low cost. Phytochemical substances obtained from plants that reduce corrosion reaction rates are termed inhibitors. The plant extract is organic in its nature, and it contains secondary-metabolized compounds such as alkaloids, amino acids, pigment, and flavonoids etc behave like inhibitors.

These types of natural products contain N, O, S, and multiple bonds so that their lone pair electrons or pi-electrons are adsorbed on the metal surface and form a protective layer to prevent metal from corrosion.

The experimental outcomes come from weight-loss study and electrochemical impedance spectroscopy studies and to support a better understanding of the adsorption of phytochemicals, computational studies were needed to operate. The quantum chemical calculations have been performed as a part of computational studies. It is well known that plant extract contains more than one phytochemical constituent. In this computational evaluation, we chose the phytochemicals present in the plant extract. The selected molecules or phytochemicals have been operated using density functional theory (DFT) using Gaussian 09 program. To decide the intensity and interaction properties of phytochemicals molecules on the metal surface Fe (110), Monte Carlo (MC), and molecular dynamics (MD) have been carried out.

2. Corrosion

Corrosion is a surface process where the oxide layer is formed on the surface of the metal. There is various types of corrosion such as oxidation corrosion, corrosion by other gases such as Cl_2, SO_2, H_2S, NO_x, liquid metal corrosion, differential metal corrosion, differential aeration corrosion, crevice corrosion, and pitting corrosion. If we discuss pitting corrosion as an example, it is due to the formation of small holes or pits on the metal surface. Pitting corrosion is highly destructive as pits are very small to be observed and usually covered with corrosion products. The pitting corrosion is the result of depassivation of a small area on the metal surface, which acts as an anode, while the rest of the undefined and large surface acts as a cathode. It is preceded by a spontaneous galvanic reaction with very limited diffusion of ions (**Figure 1**) [6].

Figure 1.
Corrosion in water pipeline.

2.1 Electrochemical aspects of corrosion

Most of the metals that we humans commonly use are unstable in the atmosphere as they were obtained from respective ores by artificial reduction through a chemical process. Thus, such metals undergo a reaction very easily to get converted into a stable form. The chemical reactions that do not require any external medium or reagent like energy or catalyst to proceed but occur on their own are called as spontaneous reactions. For spontaneous reactions, the formed products are more stable than reactants. The value for change in Gibb's free energy is always negative, and change in enthalpy is also negative, while the change in entropy is positive for such reactions.

The reactions in which oxidation and reduction both occur simultaneously are called as redox reactions. Corrosion also involves a redox reaction in which one specie or metal or part of the metal is oxidized and it acts as an anode, while the other specie or metal or part of the metal is reduced and acts as a cathode. At anode loss of electrons takes place and loss of mass occurs, while at cathode gain of electron takes place and deposition of corrosion products occurs.

The most primitive corrosion is where anodic oxidation reactions involve a pure iron when it is exposed to a strong acid such as hydrochloric acid. The reaction occurs with the formation of bubble violently. It is given as follows:

$$Fe + 2\mathrm{H}^{+} + Cl_2^{-} \rightarrow Fe^{+2} + Cl^{2-} + \mathrm{H}_2 \uparrow \quad (1)$$

$$Fe + 2\mathrm{HCl} \rightarrow \mathrm{FeCl}_2 + \mathrm{H}_2 \uparrow \quad (2)$$

Another example is the exposure of iron toward moisture or water (**Figure 2**).

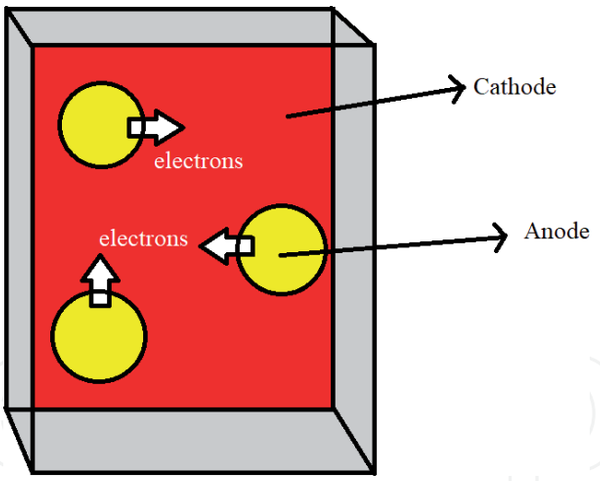

Figure 2.
Anode and cathode formation.

$$Fe \rightarrow Fe_2 + +2e^- \tag{3}$$

$$O_2 + H_2O + 4e^- \rightarrow 4OH^- \tag{4}$$

$$Fe^{2+} + 2OH^- \rightarrow Fe(OH)_2 \tag{5}$$

$$Fe^{3+} + 3OH^- \rightarrow Fe(OH)_3 \tag{6}$$

Some other reactions involve in the formation of anode and cathode that leads to corrosion are given below.

Examples of anode reactions:

$$Zn(s) \rightarrow Zn^{+2}(aq) + 2e \tag{7}$$

$$Al(s) \rightarrow Al^{+3}(aq) + 3e \tag{8}$$

$$Fe^{+2}(s) \rightarrow Fe^{+3}(aq) + e \tag{9}$$

An examples of cathode reaction:

$$H^+(aq) + e \rightarrow 1/2H_2(g) \tag{10}$$

Corrosion reactions are often electrochemical in nature. The reaction is time-consuming and may take few weeks to months to occur, it is a time and temperature-dependent reaction.

If corrosion reactions occur in aqueous media, then they are similar to that of Leclanche cell. As shown in **Figure 3**, a zinc container act as an anode, it gets oxidized. Graphite rod coated with carbon and MnO_2 paste acts as a cathode, it gets reduced, whereas both anode and cathode are joined by means of NH_4Cl and $ZnCl_2$ paste that serves the role of electrolyte. The greater the flow of electrons, the greater is the corrosion of the zinc electrode [7, 8].

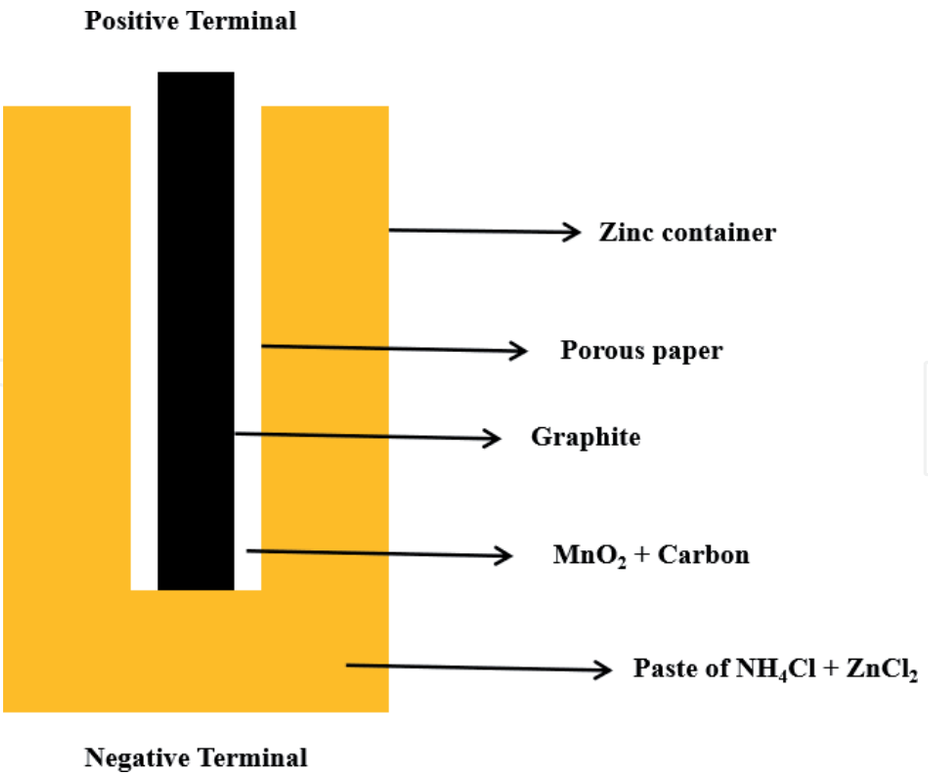

Figure 3.
Dry cell components.

2.2 Local cell formations

2.2.1 Dissimilar electrode cells

When two dissimilar metals come in direct contact with each other and an electrolytic substance is present between them, then dissimilar electrode cells are formed. It is basically a Galvanic cell, for example, we have a Daniel cell in which zinc and copper are in contact. In daily life, a copper pipe connected to a steel pipe provides an example of this type of corrosion cell. This cell is also referred to as galvanic coupling cell, the less noble metal becomes the anode whereas others act as a cathode (**Figure 4**).

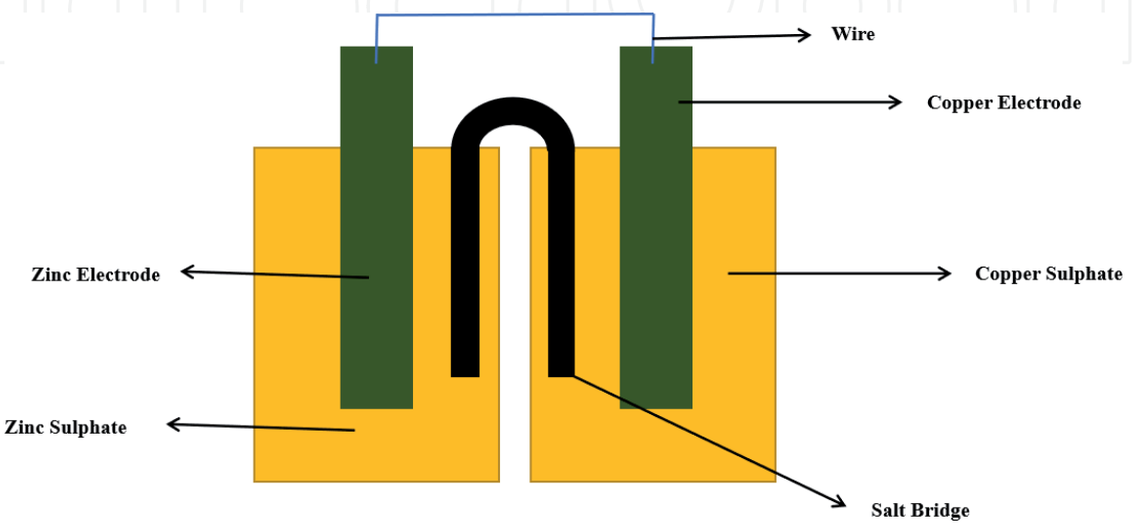

Figure 4.
Daniel cell.

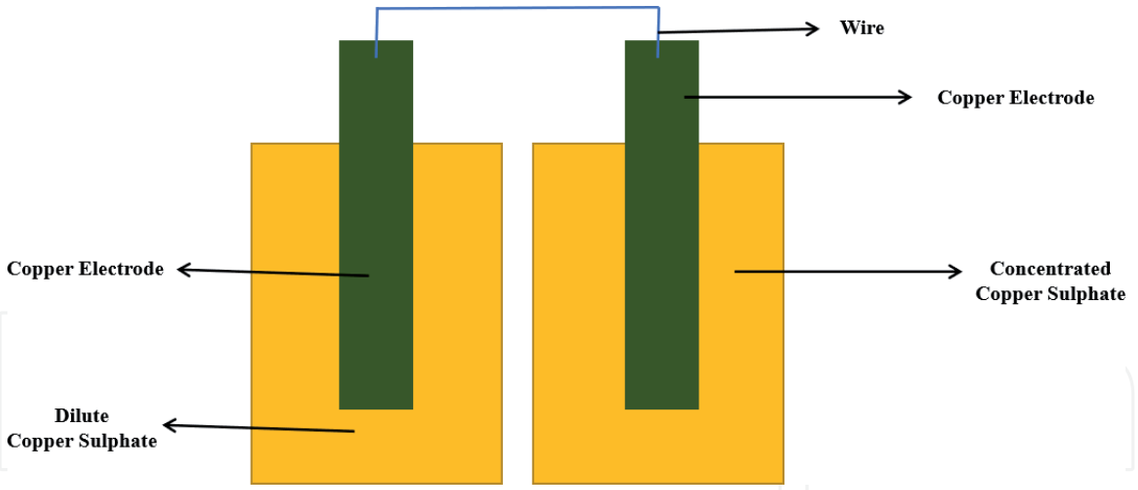

Figure 5.
Concentrated cell.

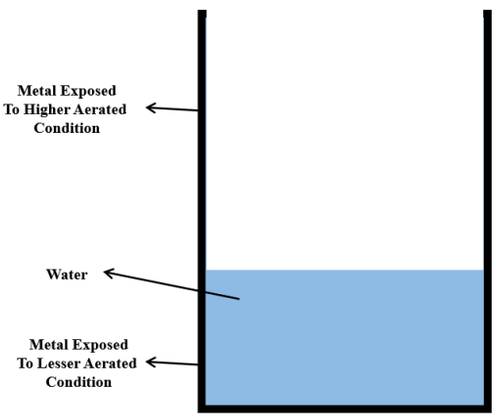

Figure 6.
Differential aeration cell.

2.2.2 Concentration cells

When two similar electrodes dipped in solutions of different compositions come in contact, then concentration cells are formed. The electrode dipped in dilute solution acts as an anode, while the electrode that is in contact with concentrated solution acts as a cathode (**Figure 5**).

2.2.3 Differential aeration cells

When two similar electrodes exposed to different aeration conditions come in contact with one another, then differential aeration cells are formed. The electrode exposed to lesser aeration conditions will act as an anode, while the electrode exposed to higher aeration conditions will act as a cathode. This type of corrosion is very common and is responsible for the significant economic loss (**Figure 6**) [9, 10].

3. Natural corrosion inhibitors

Natural corrosion inhibitors reduced or controlled the rate of corrosion by the addition of a natural product in cleaning or pickling solution. It reduces the rate of corrosion either by inhibiting oxidation at the anode or inhibiting reduction at the

cathode, or both. It forms a protective layer at the metal surface, either by physical (means electrostatic attraction between natural product and metal surface) adsorption or chemisorption (means coordination bonds between natural product and metal surface).

Studies of natural corrosion inhibitors are one of the methods for protecting metal from corrosion. So here I am discussing a specific plant *C. microphyllus* as a natural corrosion inhibitor.

3.1 Experimental studies

3.1.1 Preparation of materials

The *C. microphyllus* is a hairy herb from the *Convolvuaceae* family, which is also known as Shankhpushpi and wind weed. The leaves are linear to oblong, small, and subsessile. About 1–3 flowers are produced, which are stalked. It is easily available all over the world. *C. microphyllus* contains alkaloids kaempferol, and p-hydroxycinnamic acid as its main phytochemical constituent [11, 12]. **Figure 7** shows the image of *C. microphyllus* aerial parts and its main phytochemicals.

The soxhlet apparatus is used for plant extraction. Fresh *C. microphyllus* aerial parts were collected from our surrounding and then put them in a shaded area for few days, and after drying them properly, they were grinded to convert into powder material. Now, the powder was packed in a soxhlet apparatus and refluxed for 72 hours; then, the diluted extract was collected in the round bottom flask and transformed into a gel like extract by distillation. In the next step, the gel extract is kept in the desiccators packed with silica for few days so that the extract converts

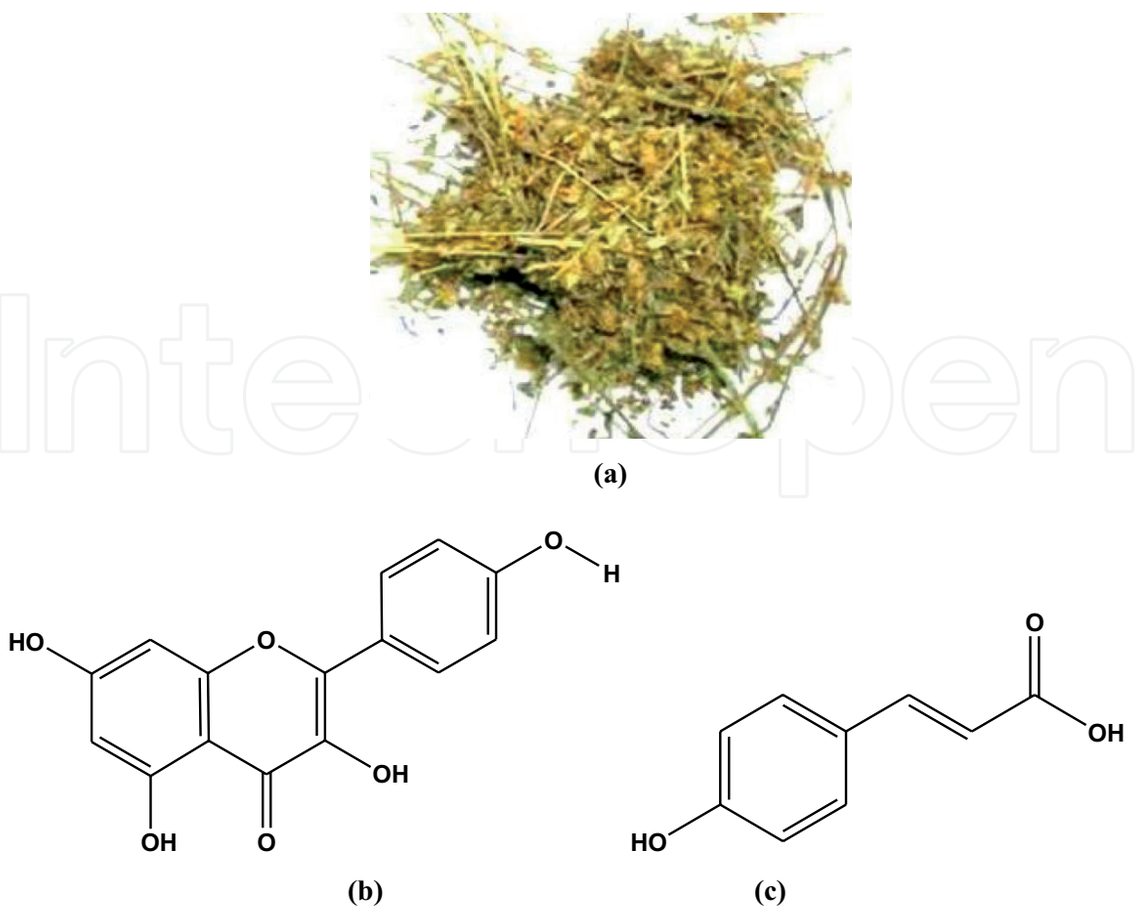

Figure 7.
(a) C. microphyllus and their main chemical components, (b) Kaempferol, and (c) p-hydroxycinnamic acid.

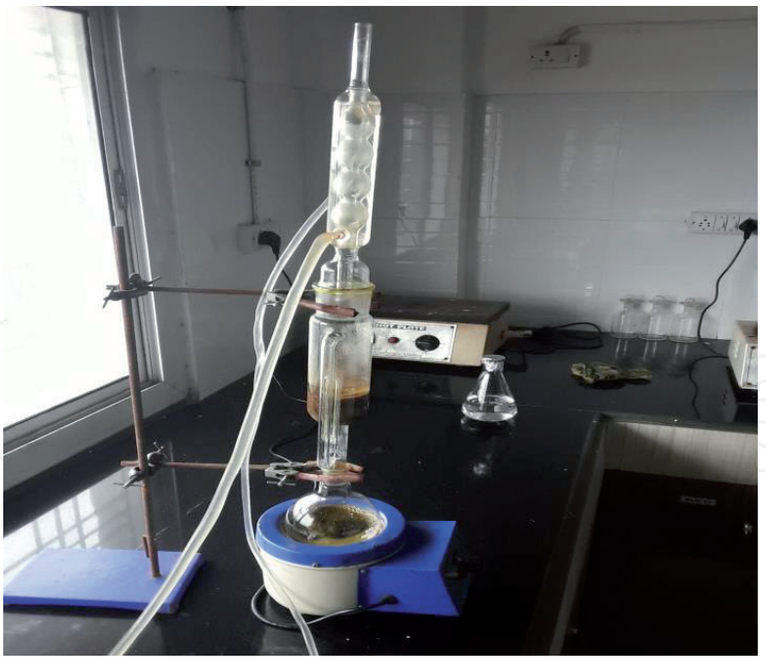

Figure 8.
Soxhlet apparatus.

Figure 9.
Desiccators.

into solid extract without moisture. After that, it is preserved in other desiccators for experimental studies.

In this work, for weight loss measurement and electrochemical impedance studies a piece of 1 cm^2 dimension is taken as a sample. These samples were mechanically polished with emery paper of different grades and subsequently cleaned with acetone, once again clean distilled water before inserting them into the pickling or cleaning solution. Here for study of *C. microphyllus* diluted solution of conc. H_2SO_4 having a molarity of 0.5 is used as a corrosive medium (**Figures 8** and **9**).

3.1.2 Weight loss studies

The best method for this measurement is the ASTM standard G 31–72 [13]. In this method, all measurements are carried out at room temperature in the thermostat.

Inhibitor concentration (mg/L)	C_R (mmy^{-1})	Efficiency (IE %)	Surface coverage Θ
0	11.33 ± 0.12	—	—
100	3.67 ± 0.17	67.55	0.6755
200	3.08 ± 0.28	72.74	0.7274
300	2.42 ± 0.37	78.59	0.7859
400	1.89 ± 0.21	83.27	0.8327
500	1.55 ± 0.31	86.31	0.8631
600	1.35 ± 0.13	88.08	0.8808

Table 1.
Corrosion rate and efficiency of mild steel in 0.5 M H_2SO_4 absence and presence of C. microphyllus for 24 hours at room temperature.

Here minimum three times repeating the same measurement for the average value. The weight loss values, surface coverage (θ), inhibition efficiency (η%), and corrosion rate (CR) are shown in **Table 1** at different concentrations of *C. microphyllus* extract for mild steel. At different concentrations of *C. microphyllus* extract, the value of weight loss, surface coverage (θ), inhibition efficiency (η%), and corrosion rate (CR) for mild steel were calculated by equations that are as follows:

$$C_R = \frac{K \times W}{A \times t \times \rho} \tag{11}$$

$$IE(\%) = \frac{C^0_{R-} C^i_R}{C^0_R} \times 100 \tag{12}$$

$$\theta = \frac{C^0_{R-} C^i_R}{C^0_R} \tag{13}$$

where,

- C_R = corrosion rate (mmy^{-1})
- W = weight loss of iron alloy (g)
- K = 8.76 × 10^4 (constant)
- ρ = 7.86 g cm^{-3} (density of Fe)
- t = immersion time (h)
- A = area of the iron alloy coupon
- θ shows surface coverage values.
- C^i_R shows the corrosion rate with inhibitor.
- C^0_R shows the corrosion rate of the iron alloy without the inhibitor.

From the above data, it is clear that the concentration of *C. microphyllus* extract is inversely proportional to the rate of corrosion, which is used as an inhibitor.

Adsorption of active phytochemicals of *C. microphyllus* extract occurs on the surface of mild steel, which reduces the surface area available for corrosion that is why the rate of corrosion decreases. The highest inhibition efficiency 88.08% is obtained at 600 mg/L.

3.1.3 Electrochemical measurements

An electrochemical workstation is used for the electrochemical measurement. The workstation is made up of three electrodes: (a) the working electrode of metal which works like anode (b) saturated calomal electrode as the reference electrode work like cathode, and (c) platinum electrode as the counter electrode for collect current. In this measurement, metal or alloy was immersed in cleaning or pickling solutions and different concentrations of *C. microphyllus* aerial part extract were added immersed for a specific time. At room temperature, the values of the open circuit potential (OCP) were noted with respect to the reference electrode. The scanning frequency from 100 kHz to 0.01 Hz is used for recording the Nyquist plot. A 5 mV signal amplitude perturbation at OCP was considered in EIS measurement. The authentic values were taken after three-time repeat measurement.

In **Figure 10** shown Nyquist plot explained that 600 mg/L *C. microphyllus* extract provided larger radius semicircles. The diameter of the capacitive loop was enlarged by increasing *C. microphyllus* extract concentration, highest at 600 mg/L explaining also the highest inhibition effect. The radiuses of the semicircles in the case of using the *C. microphyllus* extract were larger than the blank. Because of same shapes of semicircles, it means the mechanism is not change. Calculated EIS results from the following equation provided the percentage inhibition efficiency of bio-inhibitor in the electrolytes [14]:

$$IE(\%) = \frac{R_{ct} - R_{ct}^{0}}{R_{ct}} \times 100 \tag{14}$$

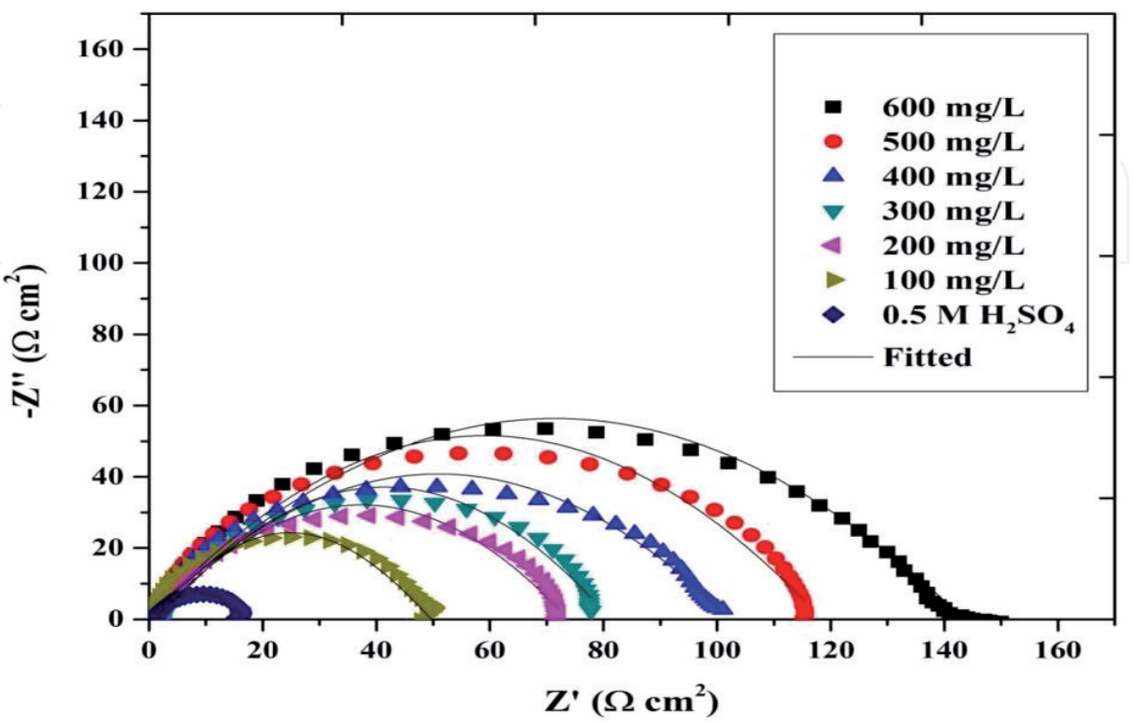

Figure 10.
Nyquist plot of mild steel in 0.5 M H_2SO_4 solution in the absence and presence of C. microphyllus extract.

Concentration of inhibitor (mg/L)	R_{ct} **(Ω cm²)**	f_{max} **(Hz)**	R_s **(Ω cm²)**	C_{dl} **(μF cm⁻²)**	N	**Efficiency (IE %)**	Θ
0	15.71	37.60	1.22	269.49	0.57	—	—
100	49.98	12.88	0.65	247.43	0.67	68.56	0.6856
200	72.58	9.46	1.63	232.19	0.68	78.35	0.7835
300	76.40	9.46	2.26	220.21	0.73	79.43	0.7943
400	104.60	7.22	0.78	211.34	0.82	84.98	0.8498
500	117.09	6.64	1.18	205.05	0.88	86.58	0.8658
600	155.13	6.64	1.68	155.15	0.91	89.87	0.8987

Table 2.
EIS parameters of mild steel in 0.5 M H_2SO_4 without and at different concentrations of C. microphyllus at 298 K.

Adsorbate	E_{HOMO}	E_{LUMO}	$\Delta E_{L\text{-}H}$	A	I	χ	H	ΔN
Hydroxycinnamic acid	−6.226	−1.996	4.230	1.996	6.226	4.111	2.115	0.1676
Kaempferol	−6.005	−2.000	4.005	2.000	6.005	4.002	2.002	0.2042

Table 3.
The HOMO and LUMO energies (eV), E_{LUMO}-E_{HOMO} energy gap ($\Delta E_{L\text{-}H}$), electron affinity (A), ionization potential (I), electronegativity (χ), hardness (η), and a fraction of electrons transferred (ΔN) for extract compounds.

where, R_{ct} and R_{ct}^0 represent the charge transfer resistance in inhibitor and blank, respectively [15].

From **Table 2**, it is clear that maximum inhibition efficiency of 89.87% was obtained at 600 mg/L of *C. microphyllus* extract, where the highest R_{ct} value was 155.13 [15]. In **Table 3**, value of the double-layer capacitor (C_{dl}) gradually decreasing means protective layer gradually form at the metal surface [16].

3.2 Computational studies

3.2.1 DFT optimization

For the evaluation of electronic features of *C. microphyllus* extract molecules (including hydroxylcinnamic acid and kaempferol shown in **Figure 11**), the structures were initially optimized by density functional theory (DFT) using Gaussian 09 program. Optimization was done *via* widely used functional of B3LYP, which was combined with 6-311G** basis function. By a combination of SCRF theory and PCM formula, these calculations were continued in the liquid phase. After optimization, the following properties were analyzed: graphics, energies, and gap of molecular orbitals of highest occupied and lowest unoccupied (HOMO, LUMO, E_{HOMO}, E_{LUMO}, and E_{LUMO}-E_{HOMO} = $\Delta E_{L\text{-}H}$) and partial charges [17].

Electronic level calculations (i.e., DFT) were performed so as to obtain insights into the reactive sites of hydroxylcinnamic acid and kaempferol molecules. The optimized hydroxylcinnamic acid and kaempferol geometries resulted from chemical DFT calculations are plotted in **Figure 11**. For these energy-minimized geometries, the analysis of frontier orbitals was done as these orbitals play a crucial role in

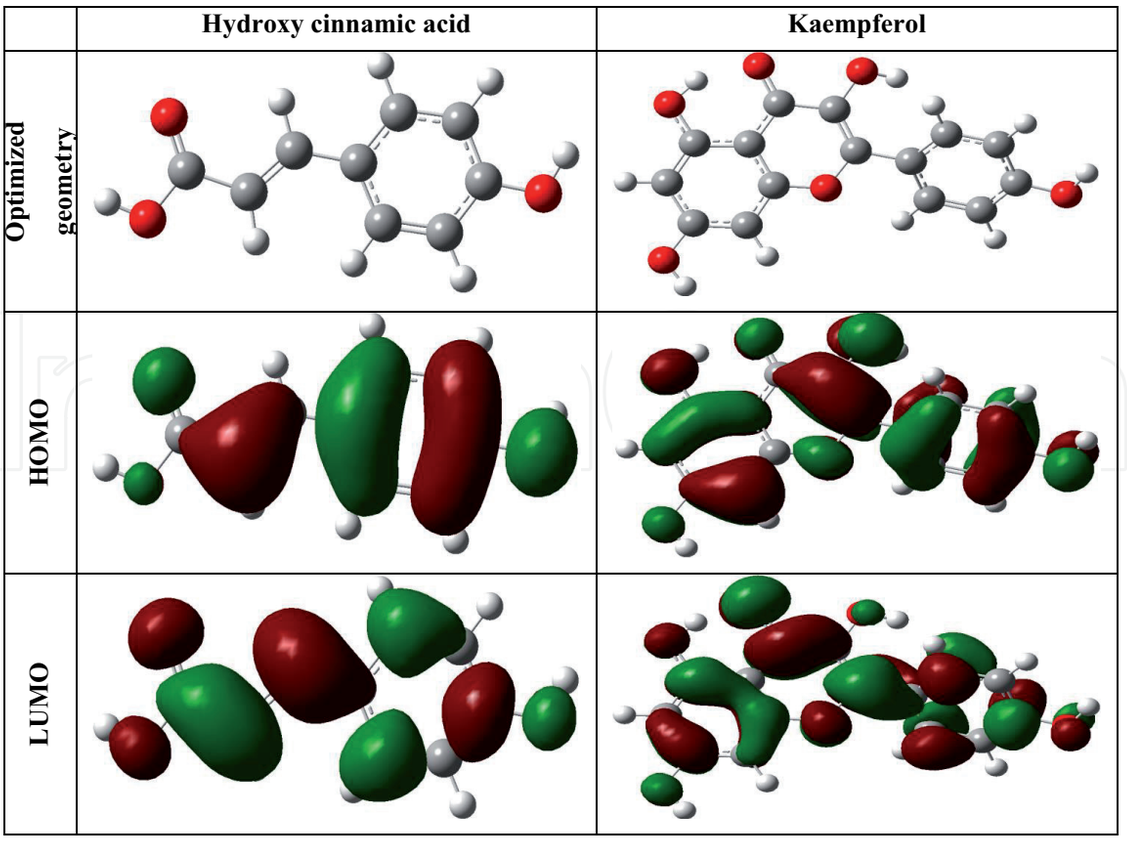

Figure 11.
*The B3LYP/6-311G** optimized geometry, HOMO, and LUMO of kaempferol and hydroxycinnamic acid compounds.*

donor-acceptor interactions of inhibiting extract molecules. The HOMO and LUMO pictures of hydroxylcinnamic acid and kaempferol are provided in **Figure 11**. As displayed, the phenyl ring, carbonyl/hydroxyl O atoms, and ethylene bond of hydroxylcinnamic acid appeared in the role of HOMO implying their strong electron supplying affinity toward a potential electron acceptor, for instance metal atoms containing unoccupied orbitals. According to the LUMO plot, all carbon and oxygen atoms of hydroxylcinnamic acid contributed to LUMO distribution, which is a signification of their tendency for getting electrons provided by filled orbitals of metal atoms. In the case of the kaempferol compound, it is seen that the HOMO placed over the entire aromatic heterocyclic skeleton and on the other hand the carbon as well as oxygen atoms behaved as reactive LUMO locations. As a consequence, the kaempferol component is able to involve in electronic interactions (i.e., donor-acceptor) with the metal surface through the donation of electrons (lone pair in hydroxyl/carbonyl O and π electrons of heterocycles) and receiving of electrons from filled iron orbitals by its C and O atoms. The eigenvalues of HOMO/LUMO and the energetic gap of frontier orbitals were examined, and the quantitative results are tabulated in **Table 3** for hydroxylcinnamic acid and kaempferol. From this table, it is evident that the kaempferol species have higher E_{HOMO} and lower E_{LUMO} in comparison with the other compound (i.e., hydroxylcinnamic acid). These results suggest the stronger electron donation and receiving capacity of kaempferol. In addition, the optimized kaempferol molecule owned a lower energetic gap ($\Delta E_{L\text{-}H}$), an observation reflecting better electron sharing and subsequent stronger corrosion inhibition manner of this compound of *C. microphyllus* extract. This trend of DFT calculated electronic parameters and simulated adsorption energies discloses the stronger kaempferol interactions and adsorption on the steel surface leading to its more effective corrosion prevention influence as compared with the inhibiting molecule of hydroxylcinnamic acid [18, 19].

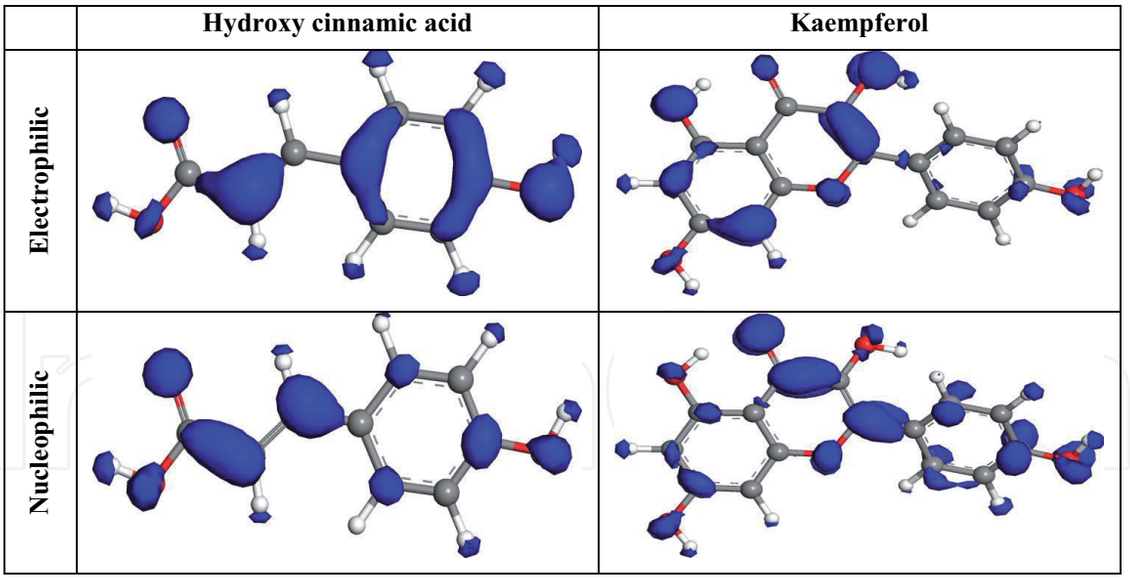

Figure 12.
The simulated Fukui indices of kaempferol and hydroxycinnamic acid compounds.

The electrophilic/nucleophilic interactions of studied molecules are summarized in **Figure 12**. From the given pictures, it is obvious that the electrophilic nature of hydroxylcinnamic acid is graphically distributed on benzene ring and double bond of carbon atoms (with a rich source of π electrons) and heteroatom of O (owing lone pair electrons). These electrons could be donated to an appropriate acceptor of electrons like metal atoms that are composed of empty orbitals. Moreover, similar to LUMO distribution, almost all carbon atoms along with three O heteroatoms are the most reactive sites for nucleophilic behavior clarifying electron getting affinity of these atomic sites. Also, the electrophilic interactions of equilibrated kaempferol compound could likely happen *via* its electron-rich places including heterocycles and the oxygen atoms of surrounding oxygenated fragments. On the other side, the O and C atoms of the whole backbone could accept electrons when attacked by a nucleophile [20, 21].

3.2.2 Molecular simulations

The hydroxylcinnamic acid and kaempferol adsorption and their interactions with the substrate (i.e., steel) were examined applying molecular simulations. These atomic simulations include Monte Carlo (MC) and molecular dynamics (MD). For the representation of steel substrate in these simulations, the frequently applied iron surface Fe (110) was used. The thickness, vacuum region, and periodic replication of this surface were set as 1.5 nm, 4 nm, and (14 × 14), respectively. To examine the adsorption preference of extract components, which are output from DFT calculations, on the iron substrate the MC-based simulation was carried out by adsorption Locator module (Materials Studio software). The MC simulations convergency was controlled with a level of fine. The last cell with the lowest potential energy generated by MC was the starting simulation box of the next modeling, that is, MD. For performing this simulation in solution phase-like experiments, water molecules were also added to the MC-generated cell. Thereafter, an optimization of 20,000 steps and NVT MD simulation of 1 ns were successively performed *via* COMPASS force field and Forcite module. The time step and temperature of NVT were set as 1 fs and 298 K. The electrostatic interactions of hydroxyl cinnamic acid and kaempferol were modeled by the Ewald scheme along with their charges calculated by DFT. The interactions of van der Waals form were evaluated by the atom-based cutoff. All metal atoms of the substrate were kept fixed [22, 23].

3.2.3 Molecular simulation

Simulations at molecular scale namely MC and MD were conducted for the analysis of the ability of *C. microphyllus* extract molecules adsorption above the metal surface (Fe (110)). The equilibrated cells of hydroxyl cinnamic acid and kaempferol generated by MC-based molecular simulations are displayed in **Figure 13**. The depicted MC snapshots clearly demonstrate that the *C. microphyllus* extract species have the ability of approaching and adsorption to iron surfaces. It is observed from the presented top views that hydroxylcinnamic acid and kaempferol adsorption on the surface happened through preferred flat orientation. The aromatic backbones of these adsorbed *C. microphyllus* extract molecules aligned parallel relative to the outmost iron atoms. The adsorption of hydroxylcinnamic acid and kaempferol took place with energies of −96.65 and − 165.51 kcal/mol, respectively. The adsorption energies of hydroxyl cinnamic acid and kaempferol with negative values further declare their adsorption over the steel substrate. The molecular adsorption was more evaluated through conducting liquid-phase dynamics (MD) simulations. The resulting snapshots of such simulations for hydroxyl cinnamic acid and kaempferol compounds are depicted in **Figure 13**. The obtained side views of ultimate simulation snapshots indicate that the chosen *C. microphyllus* extract compounds equilibrated in the vicinity of the crystalline surface (i.e., Fe (110)) under the wet conditions of the interface. This observation points to the fact that hydroxyl cinnamic acid and kaempferol as organic constituents of the green extract could bind to the surface of iron even in the presence of water molecules. Such surface adsorption affinity

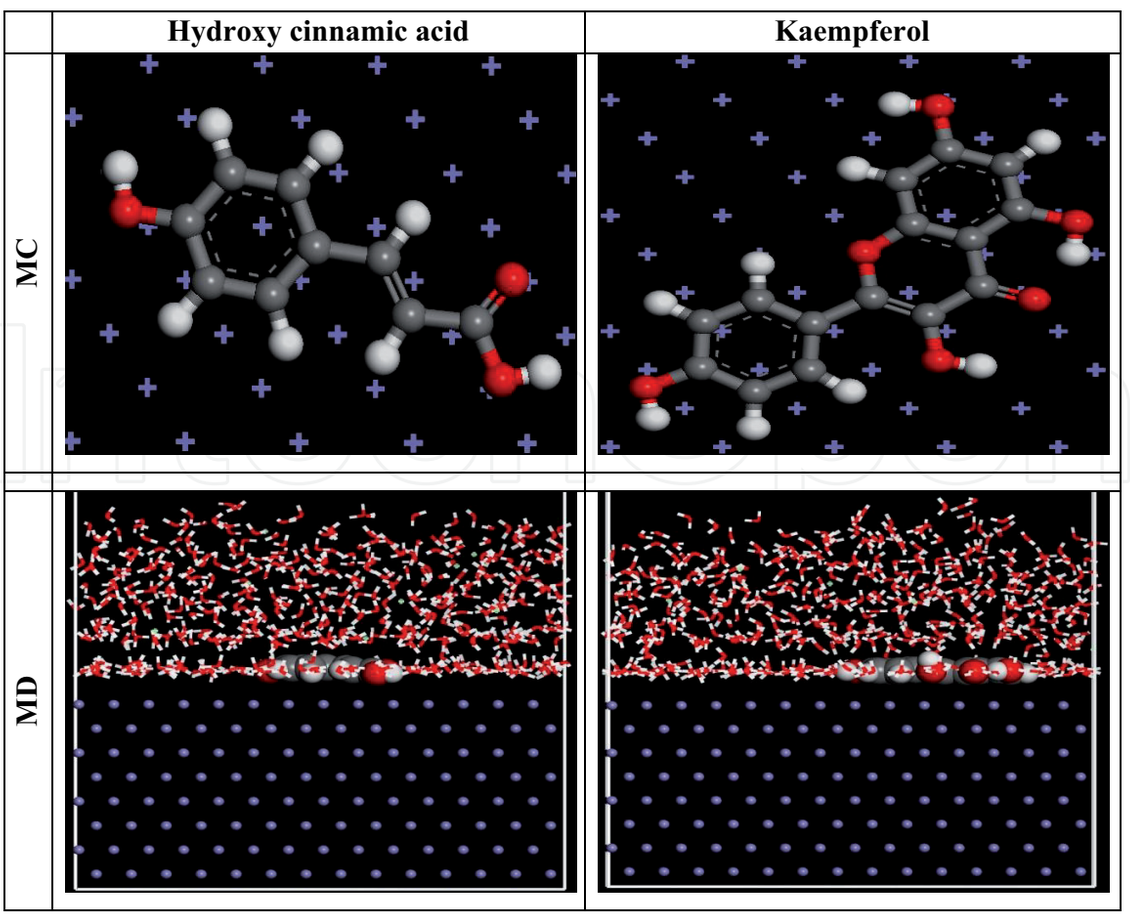

Figure 13.
The final snapshots of kaempferol and hydroxycinnamic acid compounds over Fe (110) surface obtained from MC and MD simulations.

was quantified by corresponding adsorption energy values. The energies related to hydroxyl cinnamic acid and kaempferol adsorption were estimated as −137.53 and −208.02 kcal/mol, respectively. The negative MD-calculated adsorption energies further reflect the adsorption propensity of extract components on the metallic adsorbent. In summary, the MC and MD snapshots together with predicted adsorption energies propose that the *C. microphyllus* extract compounds of hydroxyl cinnamic acid and kaempferol are capable of adsorbing on the steel substrate. The surface adsorption enables the organic extract molecules to form corrosion-preventing films over the surface, which is in support of experimental results [24, 25].

4. Conclusion

This chapter covers the corrosion problem and due to corrosion worldwide loss. This chapter discusses the importance of mild steel and discusses corrosion as a spontaneous electrochemical process. This chapter also explains of formation of different type of cells, due to different types of conditions, then start electrochemical corrosion process at the anode. In this chapter, I have discussed new developments as an example of natural corrosion inhibitor *C. microphyllus*, here I have discussed preparing inhibitors and explain experimental methods such as weight loss and electrochemical study for calculating their corrosion inhibition efficiency. After that, I have discussed computational studies of their main phytochemicals with help of DFT, molecular simulations, and molecular simulation to understand their relative adsorption properties.

Conflict of interest

The authors declare no conflict of interest.

Author details

Dwarika Prasad
Department of Chemistry, Shri Guru Ram Rai University,
Dehradun, Uttarakhand, India

*Address all correspondence to: dwarika.maithani@gmail.com

References

[1] Goyal M, Kumar S, Bahadur I, Verma C, Ebenso EE. Organic corrosion inhibitors for industrial cleaning of ferrous and non-ferrous metals in acidic solutions: A review. Journal of Molecular Liquids. 2018;**256**:565-573

[2] Verma C, Olasunkanmi LO, Ebenso EE, Quraishi MA. Substituents effect on corrosion inhibition performance of organic compounds in aggressive ionic solutions: A review. Journal of Molecular Liquids. 2018;**251**:100-118

[3] Marcus P. Corrosion Mechanisms in Theory and Practice. 3rd ed. Boca Raton, Florida: Taylor & Francis; 2011:2. DOI: 10.1201/b11020

[4] Scully JC. The Fundamentals of Corrosion. 2nd ed. USSR/Russia: International Nuclear Information System; 1978:2

[5] Haldhar R, Prasad D, Saxena A. Myristica fragrans extract as an eco-friendly corrosion inhibitor for mild steel in 0.5 M H_2SO_4. Journal of Environmental Chemical Engineering. 2018;**6**:2290-2301

[6] Fontana MG, Mitra MS. The Eight Forms of Corrosion & the Corrective Measures. India: CSIR-National Metallurgical Laboratory Jamshedpur; 1953:2-3

[7] Coleman J. Dry cell dynamics: The bobbin. Transactions of the Electro-chemical Society. 1946;**90**:545

[8] Revie RW. Corrosion and Corrosion Control: An Introduction to Corrosion Science and Engineering. Hoboken New Jersey, United States: Wiley; 2008:4

[9] Sato N. Basics of Corrosion Chemistry, Green Corrosion Chemistry. Hoboken, New Jersey United States: Wiley; 2011:6. DOI: 10.1002/9783527641789

[10] Schweitzer PA. Fundamentals of Corrosion. Boca Raton, Florida: Taylor & Francis; 2009:6. DOI: 10.1201/9781420067712

[11] Wagner H, Schwarting G. Struktur der microphyllinsaure aus dem harz von, Convolvulus microphyllus. Phytochemistry. 1977;**16**:715-717

[12] Amin H, Sharma R, Vyas M, Prajapati PK, Dhiman K. Shankhapushpi (Convolvulus pluricaulis choise): Validation of the Ayurvedic therapeutic claims through contemporary studies. International Journal of Green Pharmacy. 2014;**8**:193-200

[13] Ji G, Anjum S, Sundaram S, Prakash R. Musa paradisica peel extract as green corrosion inhibitor for iron alloyin HCl solution. Corrosion Science. 2015;**90**:107-117

[14] El-Etre AY, Abdallah M, El-Tantawy ZE. Corrosion inhibition of some metals using Lawsonia extract. Corrosion Science. 2005;**47**:385-395

[15] Joseph OO, Fayomi OSI, Joseph OO, Adenigba OA. Effect of Lecaniodiscus cupaniodes extract in corrosion inhibition of normalized and annealed mild steels in 0.5 M HCl. Energy Procedia. 2017;**119**:845-851

[16] Haldhar R, Prasad D, Bhardwaj N. Extraction and experimental studies of Citrus aurantifolia as an economical and green corrosion inhibitor for iron alloy in acidic media. Journal of Adhesion Science and Technology. 2019;**33**:1169-1183

[17] Ramezanzadeh M, Bahlakeh G, Sanaei Z, Ramezanzadeh B. Corrosion inhibition of mild steel in 1 M HCl solution by ethanolic extract of eco-friendly Mangifera indica (mango) leaves: Electrochemical, molecular dynamics, Monte Carlo and ab initio study. Applied Surface Science. 2019;**463**:1058-1077

[18] Asadi N, Ramezanzadeh M, Bahlakeh G, Ramezanzadeh B. Utilizing Lemon Balm extract as an effective green corrosion inhibitor for mild steel in 1M HCl solution: A detailed experimental, molecular dynamics, Monte Carlo and quantum mechanics study. Journal of the Taiwan Institute of Chemical Engineers. 2019;**95**:252-272

[19] Alibakhshi E, Ramezanzadeh M, Bahlakeh G, Ramezanzadeh B, Mahdavian M, Motamedi M. Glycyrrhiza glabra leaves extract as a green corrosion inhibitor for mild steel in 1 M hydrochloric acid solution: Experimental, molecular dynamics, Monte Carlo and quantum mechanics study. Journal of Molecular Liquids. 2018;**255**:185-198

[20] Sanaei Z, Ramezanzadeh M, Bahlakeh G, Ramezanzadeh B. Use of Rosa canina fruit extract as a green corrosion inhibitor for mild steel in 1M HCl solution: A complementary experimental, molecular dynamics and quantum mechanics investigation. Journal of Industrial and Engineering Chemistry. 2019;**69**:18-31

[21] Ramezanzadeh M, Sanaei Z, Bahlakeh G, Ramezanzadeh B. Highly effective inhibition of mild steel corrosion in 3.5% NaCl solution by green Nettle leaves extract and synergistic effect of eco-friendly cerium nitrate additive: Experimental, MD simulation and QM investigations. Journal of Molecular Liquids. 2018;**256**:67-83

[22] Bahlakeh G, Ramezanzadeh B, Dehghani A, Ramezanzadeh M. Novel cost-effective and high-performance green inhibitor based on aqueous Peganum harmala seed extract for mild steel corrosion in HCl solution: Detailed experimental and electronic/atomic level computational explorations. Journal of Molecular Liquids. 2019;**283**:174-195

[23] Alibakhshi E, Ramezanzadeh M, Haddadi SA, Bahlakeh G, Ramezanzadeh B, Mahdavian M. Persian Liquorice extract as a highly efficient sustainable corrosion inhibitor for mild steel in sodium chloride solution. Journal of Cleaner Production. 2019;**210**:660-672

[24] Dehghani A, Bahlakeh G, Ramezanzadeh B, Ramezanzadeh M. Detailed macro–/micro-scale exploration of the excellent active corrosion inhibition of a novel environmentally friendly green inhibitor for carbon steel in acidic environments. Journal of the Taiwan Institute of Chemical Engineers. 2019;**100**:239-261

[25] Ramezanzadeh M, Bahlakeh G, Sanaei Z, Ramezanzadeh B. Studying the Urtica dioica leaves extract inhibition effect on the mild steel corrosion in 1 M HCl solution: Complementary experimental, ab initio quantum mechanics, Monte Carlo and molecular dynamics studies. Journal of Molecular Liquids. 2018;**272**:120-136